 DOI: 10.1002/masy.200950116

Electrodeposition of Amino-Functionalized Particles in a pH Gradient: Quantitative Investigations Employing an Electrochemical Quartz Crystal Microbalance

Johanna Bünsow,[1] *Ilka-Marina Grabs,*[2] *Gudrun Schmidt-Naake,*[2] *Diethelm Johannsmann**[1]

Summary: The electrodeposition of amino-functionalized polystyrene and polybutylacrylate particles onto a gold electrode was investigated by an electrochemical quartz crystal microbalance (EQCM) and by AFM imaging. Particles with diameters in the range of 100 nm were prepared by miniemulsion polymerization. An electrochemical pH modulation in front of the electrode induced the neutralization of the amino groups and the particles readily precipitated onto the surface. The efficiency of the deposition was a function of the applied voltage, of the particles' softness, and of the amino content of the particles. Depending on the polymer composition, the coatings consisted of a dense array of individual miniemulsion particles or of a smooth polymer surface produced by coalescence.

Keywords: coatings; electrochemical quartz crystal microbalance; electrodeposition; miniemulsion; nanoparticles

Introduction

Electrochemical techniques for the coating of conducting substrates with polymer films are attractive for many applications. Often, electrochemically formed coatings serve to protect the metal substrate from corrosion.[1] Further applications are the preparation of composite materials with improved mechanical properties[2] and the production of amperometric biosensors.[3]

Numerous electrochemical methods allow for the deposition of polymer films onto conducting substrates. One can in principle distinguish between electrochemically induced *in-situ* polymerization (conceptually similar to the ''grafting-from'' technique) and electrodeposition of preformed polymers (the analog of ''grafting-to''). Note, however, that most electrochemical techniques do not produce a covalent bond between the polymer and the substrate. Examples of electrochemically triggered in-situ polymerizations are the electropolymerization of conducting polymers,[4] electrografting,[1,5,6] and electrochemically induced polymerizations where the initiating species is produced at anodic[7–11] or cathodic potentials.[12–17] In-situ polymerization is attractive because it does not require a high synthetic effort. However, it can not provide a good control over the polymer properties such as chain length, polydispersity, composition, or cross-linking density. Electrodeposition is versatile with regard to the preparation of the polymer and allows for polymer characterization prior to deposition. Here, the choice of the polymer is restricted by the need for groups that allow for the electrochemical deposition. Such

[1] Institute of Physical Chemistry, Clausthal University of Technology, Arnold-Sommerfeld-Strasse 4, 38678 Clausthal-Zellerfeld, Germany
Fax: + 49-5323-72 4835;
E-mail: johannsmann@pc.tu-clausthal.de;
[2] Institute of Technical Chemistry, Clausthal University of Technology, Erzstrasse 18D, 38678 Clausthal-Zellerfeld, Germany

groups mostly carry a charge which depends on local pH. For example, Schuhmann and co-workers precipitated anodic and cathodic electrodeposition paints.[18,19] Similarly to the electrocoating process used in car industry,[20] this method relies on the neutralization of acidic or basic polymer chains in an electrochemically induced pH gradient. In a similar approach, Sakurai et al. used the electrodeposition of aminated or carboxylated particles from a polymer emulsion at high voltages to produce microlens arrays.[21] Here, we report on experiments were an electrochemically produced pH gradient induces the neutralization and deposition of amino-functionalized miniemulsion particles. We quantitatively monitor the process with an electrochemical quartz crystal microbalance (EQCM).

In miniemulsion polymerization, an oil phase containing a monomer is emulsified in water by application of shear.[22,23] The droplets obtained by emulsification are stabilized by a surfactant and a ''hydrophobe'', that is, a substance which is completely insoluble in water and therefore prevents Ostwald ripening. Initiation of a free-radical polymerization solidifies the droplets and yields monodisperse polymer particles with diameters in the range of around 100 nm. Miniemulsion polymerization can be applied to a broad range of monomers and allows for the formation of complex architectures.[24,25]

Experimental Part

Preparation of Particles

The preparation of amino-functionalized particles was in detail described in reference.[26] Briefly, the particles were prepared by copolymerization of styrene or butylacrylate with 2-aminoethyl methacrylate hydrochloride (AEMA) in a miniemulsion process. Cetyltrimethylammonium bromide was used as cationic surfactant and hexadecane as the hydrophobic agent. The polymerization was started in the oil phase with 2,2′-azobisisobutyronitrile to prevent polymerization of the amino-monomer in the aqueous phase. The monomer-to-water ratio was 1:8 and the AEMA content in the feed mixture was either 10 or 20 mol-%. When referring to these amino contents as ''10%'' or ''20%'' below, we do not mean to imply that these ratios would apply to the amount of amino groups at the particle surface. This amount a priori is not known.

After preparation, the latex samples were cleaned by repetitive centrifugation/redispersion in deionized water. Particle sizes were in the range of 100 nm as determined by dynamic light scattering (DLS) using photon cross-correlation spectroscopy (PCCS, Nanophox, Sympatec, Germany).

Electrodeposition of Amino-Functionalized Particles

Electrodeposition was carried out with polystyrene and polybutylacrylate miniemulsions with a content of either 10 or 20% amino groups. To render the solution conductive, 0.25 mol/L ammonium sulphate were added as the supporting electrolyte. In most cases, the miniemulsions were diluted in a ratio of 1:1 with 0.25 M aqueous ammonium sulphate solution. Sometimes, the dilution was omitted. Standard experiments were performed with a diluted miniemulsion of polystyrene particles with an amino content of 20% in a potential range from 0 to −2 V. The deposition was performed in a three-electrode setup with the gold front electrode of a 5 MHz quartz crystal (Maxtek, Santa Fe Springs, CA) as the working electrode, a platinum ring as the counter electrode, and a saturated calomel reference electrode (SCE, Sensortechnik Meinsberg, Germany). All potentials were measured relative to SCE. Cyclovoltammograms were acquired with a potentiostat (IviumStat, EKTechnologies, Germany) in a potential range from 0 to −1.2 V or 0 to −2 V with a ramp rate of 100 mV/s. The shifts of frequency and half bandwidth at half maximum (bandwidth, for short) were detected in-situ with a network analyzer (HP4396A, Hewlett Packard). Resonance parameters were inferred from the spectra by impedance

analysis. The frequency shifts were converted to a film thickness using the Sauerbrey equation

$$\Delta f = -\frac{2nf_f^2}{Z_q} m_S = -\frac{2nf_f^2}{Z_q} \rho_f d_S, \quad (1)$$

where f_f is the frequency of the fundamental, n is the overtone order, $Z_q = 8.8 \times 10^6$ kg m^{-2} s^{-1} is the acoustic impedance of AT-cut quartz, m_S is the mass per unit area of the film, $\rho_f = 1$ g cm^{-3} is the density of the film, and d_S is the film thickness in the Sauerbrey sense. When the quartz is operated in a liquid environment, the Sauerbrey equation often does not yield the geometric thickness because surface roughness, trapped solvent, and the product of density and viscosity of the bulk liquid contribute to the frequency shift. In the case reported here, the formation of hydrogen bubbles at negative potentials further complicates the situation.

All samples were extensively rinsed with water after electrodeposition and stored in ultrapure water (arium 611VF, Sartorius, Germany) at room temperature.

AFM Imaging

The 5 MHz quartz crystals were too large for the sample compartment of the AFM available to us. This required the preparation of separate samples for AFM imaging. The substrates used were small glass slides (1 cm × 1 cm) covered with gold and thin layer of chromium underneath, acting as an adhesion promoter. The electrodeposition was performed according to the procedure described above. All images were acquired by operating the AFM (extended multimode, NanoScope IIIa controller, Veeco/Digital Instruments) in tapping mode in air.

Results

Figure 1 shows a data set measured with an electrochemical quartz crystal microbalance (EQCM) during the deposition of amino-functionalized polystyrene particles. In this particular experiment, the amino

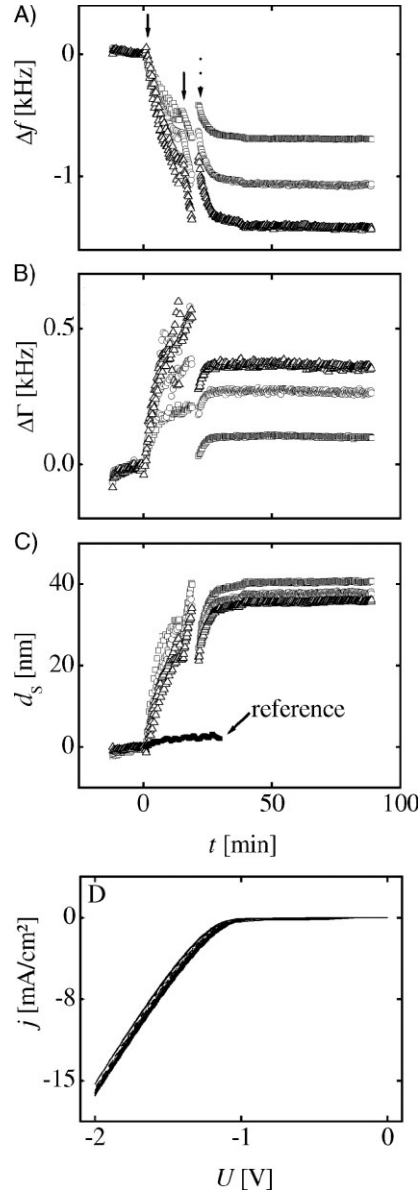

Figure 1.
Shifts of frequency (Δf, A), and bandwidth (ΔΓ, B), both measured on the 15 (squares), 25 (circles), and 35 MHz (triangles) overtone, film thickness calculated from Δf (d_S, C), and cyclovoltammograms (current density, j, D) acquired during the electrodeposition of amino-functionalized polystyrene particles. The filled squares in panel C represent a reference experiment (measured on the 15 MHz overtone) where the quartz was stored in the emulsion without application of a potential. Straight and dotted arrows indicate the range where cyclovoltammograms were acquired and rinsing with water, respectively.

content was 20% and the miniemulsion was diluted in a ratio of 1:1. The frequency (panel A) dropped rapidly when the acquisition of the cyclovoltammograms was started (arrows in panel A). Cyclic voltammetry in the range of 0 to −2 V (panel D) causes the reduction of water in front of the electrode surface and shifts the pH to the basic range. The amino-functionalized particles are neutralized in this pH gradient and precipitate onto the electrode surface. After the voltage was switched off (straight arrow in panel A) the deposition continued. Rinsing with water stopped the deposition (dotted arrow in panel A). Clearly, there are some slow follow-up processes which persist for some time even in the absence of a voltage. These may include slow transport of ions from the electrode to the bulk or slow coalescence.

The film thickness (panel C) as calculated by the Sauerbrey equation (equation 1) was 38 nm and 29 nm in the reactant solution and in air, respectively. The wet thickness is only a non-quantitative measure of the deposited mass because it contains contributions from trapped solvent, roughness, and hydrogen bubbles produced upon water decomposition. Figure 1 C also shows a reference experiment where the quartz was immersed in the miniemulsion without application of a voltage. The film had a thickness of 3 nm which was small compared to the electrochemically produced films. The formation of a thin film even in the absence of a pH gradient indicates that the particles slightly adsorb to gold. The decrease of frequency was accompanied by an increase of bandwidth (panel B) which is a measure of dissipative losses caused by the film. Presumably, the particles deposit in a loosely packed structure which contains a large amount of trapped solvent and exhibits a rough surface. These effects can cause a large dissipation, as observed in panel B. The cyclovoltammograms which serve to induce the pH gradient are depicted in panel D. The current densities are large at potentials below −1 V, where the decomposition of water takes place. An enlarged image of the hydrogen current at −2 V is given in Figure 2. These particular cyclovoltammograms were acquired during the preparation of a sample for AFM imaging. For the reason of clarity, we just show some selected scans. The decrease of the current in consecutive scans (10 mA in 20 scans) proves that the surface becomes covered by a film. Hydrogen evolution is hindered at those locations, where polymer particles stick to the surface.

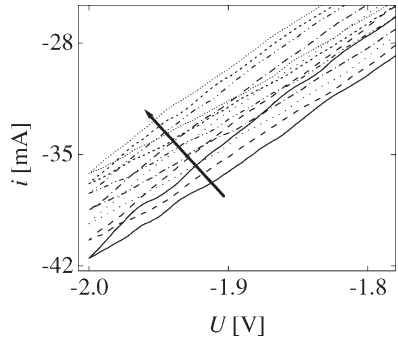

Figure 2.
Zoom into hydrogen peak in cyclovoltammograms acquired during the electrodeposition of amino-modified polystyrene particles onto AFM gold substrates. The arrow indicates the progress of deposition. The decrease of the peak current proves that a coating covers the electrode. For clarity, the graph just shows scans n° 2, 4, 6, 8, 12, 16, and 20. The arrow indicates the increasing number of scans.

The impact of variations of the reaction conditions on the dry film thickness is illustrated in Figure 3. When amino-functionalized polybutylacrylate particles were used rather than polystyrene particles, the dry film thickness increased strongly from 29 to 127 nm (panel A). Presumably, this increase can be explained by the different chemical nature of polystyrene and polybutylacrylate particles. Polybutylacrylate is a soft polymer whereas polystyrene forms hard particles. Packing of the softer polybutylacrylate particles will result in a much denser structure due to deformation of the particles (compare Figure 4 C) which results in a larger film thickness. Further variations were all carried out with polystyrene particles.

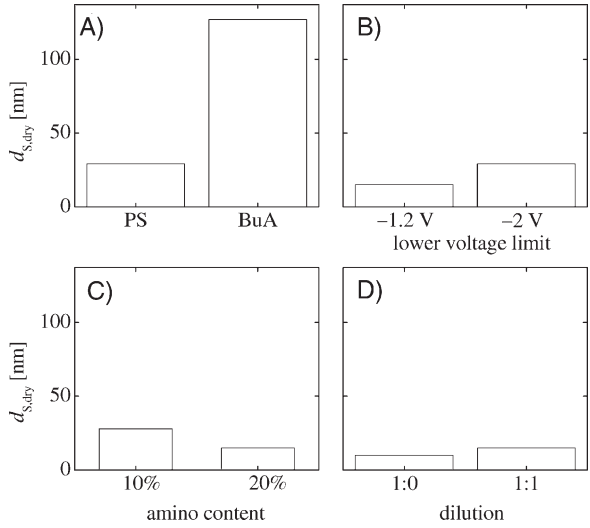

Figure 3.
Influence of the type of particle (A: polystyrene, PS, or polybutylacrylate, BuA), of the potential range (B), of the amino content (C) and of the dilution of the miniemulsion (D) on the dry film thickness $d_{S,dry}$ of the coating in air. Standard experiments were performed with PS particles with an amino content of 20% at a dilution of 1:1 by varying the potential from 0 to −2 V with 100 mV/s for 20 times.

When the range of the cyclovoltammograms was extended from −1.2 to −2 V (panel B), the film thickness increased. The increase in thickness is related to a larger pH gradient where more particles become neutralized and precipitate onto the electrode. An increase of the amount of amino groups of the particles decreases the film

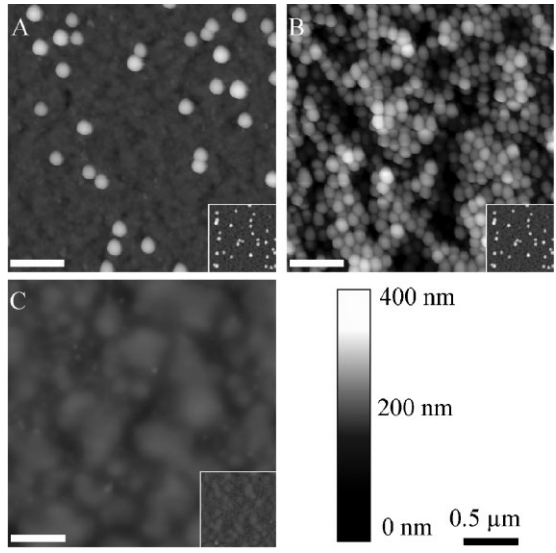

Figure 4.
AFM images acquired on electrodeposited amino-modified polystyrene (A,B) or polybutylacrylate (C) particles with a lower voltage limit of −1.2 (A) or −2 V (B, C). The amino content was 20%. The dispersion was diluted with water in a ratio 1:1. The insets represent reference samples produced by immersion of a gold substrate into the miniemulsion without application of a voltage.

thickness (panel C). Clearly, a larger amount of amino groups increases the pK_A of the particles.

A larger pH gradient would be required to deposit the same amount of material as compared to particles with a lower pK_A. Dilution of the miniemulsion with water slightly *in*creased the film thickness (panel D). Usually one would expect the opposite. However, the difference in thickness was 5 nm which is close to the experimental error. Presumably, the pH gradient as determined by the applied potential and the amount of amino groups dominate the film thickness of a given miniemulsion.

AFM images were acquired on electrodeposited films as illustrated in Figure 4. The insets represent reference samples prepared by dip-coating followed by rinsing with copious amounts of water. The polystyrene samples (panel A and B) show globular features which are deposited particles. At an amino content of 20% (panel A), some polystyrene particles with diameters of 100 nm were imaged on a smooth surface. This surface was not the bare gold. Presumably, organic material deposits on the electrode. Such a material may be the surfactant or coalesced miniemulsion particles. The surface morphology of the reference sample is very similar to the electrodeposited sample although the film thickness was significantly higher in the latter case. We assume that a smooth organic film forms in both cases but the thickness of this film is increased by application of a potential. When the deposition was carried out at more negative potentials (panel B), a dense array of individual polystyrene particles formed. The polybutylacrylate samples (panel C) did not exhibit any features that can be attributed to single particles. Film formation dominates the surface morphology, here.[27] The morphology of the sample prepared by electrodeposition resembles the reference sample but the areas that are free of boundaries are significantly larger. Electrodeposition seems to enhance film formation.

Conclusions

Gold electrodes were coated by electrodeposition of amino-functionalized polystyrene and polybutylacrylate particles from a miniemulsion. The particles readily deposited onto the electrodes when cyclovoltammograms were acquired between 0 and −1.2 or −2 V. The film thickness ranged from 10 to 130 nm. The thickness increased with the softness of the particles, with increasing pH gradient, and with decreasing amino content of the particles. The surfaces of polystyrene samples showed loose or dense arrays of 100 nm particles. The polybutylacrylate samples exhibited a very smooth surface morphology which we ascribe to coalescence of the particles. Film formation was enhanced by electrodeposition, here.

Acknowledgements: This work has been partly funded by the European Graduate School on Microstructural Control in Free-Radical Polymerization.

[1] N. Baute, C. Jérôme, L. Martinot, M. Mertens, V. M. Geskin, R. Lazzaroni, J.-L. Brédas, R. Jérôme, *Eur. J. Inorg. Chem.* **2001**, 1097.
[2] J. P. Bell, A. S. Wimolkiatisak, H. W. Rhee, J. Chang, R. Joseph, W. Kim, D. A. Scola, *J. Adh.* **1995**, *53*, 103.
[3] W. Schuhmann, *Rev. Mol. Biotechnol.* **2002**, *82*, 425.
[4] L. B. Groenendaal, F. Jonas, D. Freitag, H. Pielartzik, J. R. Reynolds, *Adv. Mater.* **2000**, *12*, 481.
[5] S. Palacin, C. Bureau, J. Charlier, G. Deniau, B. Mouanda, P. Viel, *ChemPhysChem* **2004**, *5*, 1468.
[6] G. Deniau, J. Charlier, B. Alvado, S. Palacin, P. Aplincourt, C. Bauvais, *J. Electroanal. Chem.* **2006**, *586*, 62.
[7] N. Yamazaki, *Adv. Polymer Science* **1969**, *6*, 377.
[8] S. Yoshizawa, Z. Takehara, Z. Ogumi, C. Nagai, *J. Appl. Electrochem.* **1976**, *6*, 147.
[9] G. Yildiz, H. Çatalgil-Giz, F. Kadirgan, *J. Appl. Electrochem.* **2000**, *30*, 71.
[10] S. K. Samal, B. Nayak, *J. Polym. Sci A* **1988**, *26*, 1035.
[11] G. L. Collins, N. W. Thomas, *J. Polym. Sci.* **1977**, *15*, 1819.
[12] G. Parravano, *J. Amer. Chem. Soc.* **1951**, *73*, 628.
[13] C. S. Lee, J. P. Bell, *J. Mater. Sci.* **1995**, *30*, 3827.
[14] S. L. Cram, G. M. Spinks, G. G. Wallace, H. R. Brown, *J. Appl. Polym. Sci.* **2003**, *87*, 765.
[15] J. Reuber, H. Reinhardt, D. Johannsmann, *Langmuir* **2006**, *22*, 3362.
[16] J. Bünsow, D. Johannsmann, *Macromol. Symp.* **2007**, *248*, 207.

[17] J. Bünsow, D. Johannsmann, *J. Colloid Interf. Sci.* **2008**, *326*, 61.
[18] B. Ngounou, S. Neugebauer, A. Frodl, S. Reiter, W. Schuhmann, *Electrochim. Acta* **2004**, *49*, 3855.
[19] S. Reiter, D. Ruhlig, B. Ngounou, S. Neugebauer, S. Janiak, A. Vilkanauskyte, T. Erichsen, W. Schuhmann, *Macromol. Rapid Commun.* **2004**, *25*, 348.
[20] K. Arlt, *Electrochim. Acta* **1994**, *39*, 1189.
[21] Y. Sakurai, S. Okuda, H. Nishiguchi, N. Nagayama, M. Ykoyama, *J. Mater. Chem.* **2003**, *13*, 1862.
[22] F. J. Schork, Y. Luo, W. Smulders, J. P. Russum, A. Butté, K. Fontenot, *Adv. Polym. Sci.* **2003**, *175*, 129.
[23] K. Landfester, *Macromol. Rapid Commun.* **2001**, *22*, 896.
[24] T. Kiezke, D. Neher, M. Kumke, O. Ghazy, U. Ziener, K. Landfester, *Small* **2007**, *3*, 1041.
[25] A. Guyot, K. Landfester, F. J. Schork, C. Wang, *Prog. Polym. Sci.* **2007**, *32*, 1439.
[26] I.-M. Grabs, G. Schmidt-Naake, *Macromol. Symp.*, *this issue.*
[27] J. L. Keddie, *Mater. Sci. Eng. R* **1997**, *21*, 101.

